Journal of the Brazilian Society of Mechanical Sciences and Engineering (2024) 46:519
https://doi.org/10.1007/s40430-024-05091-7

TECHNICAL PAPER

Toward enhanced mechanical rigidity: additive manufacturing of auxetic tubes with PU core and comparative analysis of unique structural behaviors

Rhuan José Ribeiro Pereira[1] · Rafael Augusto Gomes[1] · Guilherme Ferreira Gomes[1]

Received: 28 January 2024 / Accepted: 13 July 2024 / Published online: 30 July 2024

Abstract

The pursuit of enhancing manufacturing and production processes has given rise to Additive Manufacturing, a methodology characterized by the production of polymeric, metallic, or composite components with high precision, commonly referred to as three-dimensional printing technology (3D printing). Currently gaining momentum across various sectors, 3D printing is favored for its streamlined production using CAD models in software, finding applications in health, structural and numerical optimization, industrial and construction, automotive, aerospace, and other fields. Furthermore, in the realm of advanced materials, research aims to discover unique structures with noteworthy properties. Auxetic structures, notable for their negative Poisson's ratio, present a characteristic that diverges from conventional materials, showcasing volumetric expansion under tensile forces, in contrast to the contraction experienced by conventional materials. This study endeavors to fabricate auxetic tubes filled with a PU core using Additive Manufacturing and subject them to compression tests. The mechanical test responses will be analyzed and compared with existing literature to assess the enhancement in mechanical rigidity without a significant increase in structural weight. Results indicate that the re-entrant structure yielded the best outcomes, with an energy absorption ratio of 1.08 J/g and an incremental ratio of 23.59, correlating the percentage increase in energy absorption with the percentage increase in mass. Additionally, unexpected behaviors were observed in certain structures: the anti-trichiral structure exhibited a Zero Poisson Ratio (ZPR) behavior, and the dragonfly structure, while inconclusive, leaned toward a ZPR behavior due to the foam diminishing the auxetic effect of the structure.

Keywords Additive manufacturing · Auxetic structures · Auxetic cell · Reentrant cell · Anti-trichiral cell · Dragonfly cell

List of symbols

D_{ext} (mm)	External diameter
D_{int} (mm)	Internal diameter
L (mm)	Length
T (mm)	Edge thickness
N_h (–)	Number of cells (horizontal)
N_v (–)	Number of cells (vertical)
t_{cell} (mm)	Thickness between cells
T_{print} (°C)	Printing temperature
T_{bed} (°C)	Bed temperature
V_{print} (mm/s)	Printing speed
H_{layer} (mm)	Layer height
ρ_{fill} (%)	Fill density
$M_{material}$ (–)	Printing material
m (g)	Mass
m_{PU} (g)	Mass with PU
Δm (%)	Increase in mass
δ (mm)	Displacement
F (N)	Force
F_{spec} (N/g)	Specific force
EA (J)	Absorbed energy
SEA (J/g)	Specific absorbed energy
MCF (N)	Main crush force

Technical Editor: Jovana Jovanova.

✉ Guilherme Ferreira Gomes
guilhermefergom@unifei.edu.br

[1] Mechanical Engineering Institute, Universidade Federal de Itajubá, Itajubá, Brazil

1 Introduction

In the realm of advanced materials engineering, the quest for structures with unique properties has been an ongoing endeavor. In this context, auxetic structures have gained prominence due to their remarkable ability to undergo volumetric expansion when subjected to tensile forces. This distinctive characteristic contrasts with the conventional behavior of materials, which typically contract when stretched.

Roderic Lakes [12] was among the first authors to observe the peculiar characteristic of auxetic materials, attributing it to the fact that these materials possess a negative Poisson's ratio. In order to avoid the cumbersome phrase "material with a negative Poisson's ratio," the term auxetic was adopted, derived from the Greek word *auxetos*, meaning "that which can be increased" [4]. The application of auxetic structures has been studied in various fields such as civil engineering [7], aerospace [19, 20], mechanical and automotive engineering [19, 20], among others.

On the other hand, in the landscape of modern manufacturing, Additive Manufacturing (AM), also known as 3D printing, has emerged as a revolutionary technique challenging traditional production approaches. This innovative approach enables the construction of three-dimensional objects through the successive deposition of material, layer by layer, based on a digital model.

AM transcends the limitations of conventional manufacturing, offering numerous advantages such as the ability to produce complex parts in a single form without the need for joints, excellent potential for surface finish depending on the specific technology used, relatively low energy consumption compared to traditional manufacturing processes, and high dimensional accuracy which can vary based on the selected manufacturing technique. The process is simplified, encompassing CAD model creation, printing, and part installation. Additionally, AM enables direct manufacturing without the need for molds, thus reducing material waste and enhancing efficiency [1]. Since its inception, 3D printing technology has evolved significantly and is now utilized across various industrial sectors, including healthcare [3, 22], automotive and aerospace [14], and civil engineering [17].

Given the widespread use of auxetic materials alongside the evolution of additive manufacturing processes, this work aims to contribute to the literature on auxetic structures and to compare three adopted auxetic structure types: reentrant, dragonfly, and anti-trichiral. The chapters discuss existing research and potential gaps to be addressed on the subject, focusing on the benefits of implementing auxetic structures in different sectors and their integration with 3D printing. The study aims to analyze the effect of PU foam filling in an auxetic tube, expecting an improvement in the potential weight-to-mechanical stiffness ratio of auxetic tubes, while also serving as a foundation for future studies.

The pursuit of innovative mechanical properties, such as tension-induced expansion observed in auxetic structures, is a promising research field poised to impact various industrial sectors, including healthcare, automotive, aerospace, and civil engineering. Auxetic structures exhibit unique characteristics such as negative Poisson's ratio, which can enhance mechanical performance in applications requiring superior energy absorption, flexibility, and resistance to fracture. This work explores the nature of auxetic structures, examining their distinctive characteristics and potential applications across these key sectors.

Additive Manufacturing has redefined manufacturing paradigms, offering a versatile and agile approach to creating complex and functionally optimized parts. This work specifically focuses on optimizing the weight-to-mechanical stiffness ratio of the final part using advanced Additive Manufacturing techniques.

Thus, this work aims to contribute to the literature on the topic by comparing the mechanical properties of auxetic tubes filled with PU foam and unfilled auxetic tubes. Additionally, the study seeks to inspire further research in the field. The central objective of this work is to analyze the effect of PU foam filling in an auxetic tube, where its energy absorption is significantly increased without a significant increase in its structural weight. This study also aims to pave the way for future research into the development of materials with advanced properties and innovative applications.

1.1 State of art

Auxetic structures can be combined with a filling core. Such a combination can be justified by the external diameter providing load-bearing capacity, while the internal core provides energy absorption capacity.

Mohsenizadeh et al. [15] encompasses experimental and numerical approaches to analyze the compression responses and energy absorption performance of auxetic foams and tubes filled with these auxetic foams. This analysis was conducted under both quasi-static and dynamic conditions. The study compares three different types of structures: hollow square tubes, tubes with conventional foams, and tubes filled with auxetic foam. The results indicate a significant relationship between the degree of auxeticity in the foam filling and the impact resistance performance of structures filled with these foams. The "degree of auxeticity" refers to the extent to which the foam exhibits negative Poisson's ratio behavior, meaning it expands laterally when compressed longitudinally. It was observed that an increase in the auxeticity level of the foam filling enhances the impact resistance performance of foam-filled structures under both quasi-static and dynamic conditions.

In the realm of auxetic materials, Jiang et al. [8] dedicated a study to analyze low-velocity impact tests, focusing on structures with an orthogonal arrangement characterized by the auxetic effect. The study compared these auxetic composites with non-auxetic composites made from the same raw materials but adopting different reinforcement configurations. Both auxetic and non-auxetic composites demonstrated sensitivity to the deformation rate, but a clear discrepancy in the mechanical responses of the two structures was evident. This difference was attributed to the distinct deformations and damage mechanisms of each category.

Similarly, Jin et al. [9] proposed a honeycomb sandwich structure composed of reentrant auxetic cells. The study focused on the dynamic responses of the structure and its resistance to explosive loads. Numerical simulations using LS-DYNA® software revealed that honeycomb structures with thicker walls demonstrated higher specific energy absorption capacity under compressive loads. The results suggested that sandwich structures exhibit greater deformation resilience when subjected to forces along the longitudinal direction (Y-axis) compared to the transverse direction (X-axis).

Additionally, Novak et al. [16] conducted research on chiral auxetic structures manufactured from Ti6Al4V alloy. These structures underwent experimental tests under both quasi-static and dynamic compression conditions. The empirical results were utilized to validate computational models developed for auxetic structures in LS-DYNA® software. The study also included an analysis of composite panels filled with an auxetic core, subjected to explosive loadings and investigated through computational simulations, evaluating maximum panel displacement and specific energy absorption. The assessment of explosive loads employed three distinct methodologies: ConWep, Smooth Particle Hydrodynamic, and Multi-Material Arbitrary Lagrange Eulerian. The analyses indicated that, in most scenarios, the impact of the chiral unit cell's amplitude on maximum displacement and specific energy absorption was relatively insignificant when contrasted with the effect of cell length.

Recent advancements in composite materials have demonstrated significant potential in enhancing mechanical properties through innovative structural designs. One notable development is the tubular composite structure analyzed by Jopek [11] which combines two materials with distinct Young’s moduli. The Young’s modulus of one material can be controlled by external conditions such as magnetic or electric fields and temperature. This study highlights how the auxetic re-entrant honeycomb cellular structure influences the behavior of a stretched tube, allowing for cross-sectional changes during deformation. Additionally, another study by Jopek [10] investigates a two-phase fibrous composite subjected to non-uniform bending loads. This composite features a matrix with a constant positive Poisson’s ratio and fibers with tunable Poisson’s ratios, ranging from positive to negative values. Using FEM analysis, the study explores the impact of fiber arrangement, volume fraction, and load distribution on the composite’s rigidity and indentation resistance. The findings confirm that auxetic reinforcement can significantly reduce deformation in the direction of the applied force, thereby enhancing the composite's mechanical performance.

Airoldi et al. [2] study precisely addresses this integration, evaluating a hexaquiral polymeric structure manufactured through 3D printing, filled with polyurethane foam inserts, and subjected to analyses under both quasi-static and dynamic conditions. Results indicated that the energy absorbed by the synergistic combination of the auxetic framework and foam is substantially higher than the sum of energies absorbed by the individual components tested in isolation. Additionally, a numerical approach was developed to handle foam-filled absorbers and underwent a validation process.

Ren et al.'s studies [18], rigid PU foams and stainless steel auxetic tubes with different geometric parameters were fabricated, and the foams were subsequently inserted into the hollow tubes to study energy absorption. The tubular types and the effects of parameters, including wall thickness and ellipticity, in tubes filled with rigid PU foam were numerically analyzed using validated models. The results show that the total energy absorbed by tubes filled with rigid PU foams is greater than the sum of simple foams and the hollow auxetic tube under compression. Geometric parameters such as wall thickness and ellipticity have a considerable effect on structural deformation mode and energy absorption.

A recent study by Liu et al. [13] involves the fabrication of composite auxetic structures filled with foam through hot molding, bonding, and agitation foaming. The study aims to analyze the responses to ballistic impact tests and the effect of foam filling. Ballistic impact test results indicated that compared to unfilled auxetic structures, the ballistic limit velocity of foam-filled auxetic structures increased by 6.12%, and the energy absorption property of foam-filled auxetic structures was improved. Furthermore, an increase in the relative density of foam had a positive effect on enhancing the anti-penetration performance of composite auxetic structures filled with foam.

With the theoretical foundation established, this work seeks to complement the literature on auxetic materials and additive manufacturing, exploring their combined implementation possibilities. This complementation will involve a comparison between different auxetic unit cells studied here and a comparison between the present study and an external work that analyzed unfilled auxetic tubes. Such a comparison can serve as a basis for future studies and diverse applications.

2 Auxetic structures

Lakes [12] was one of the pioneers in developing structures exhibiting the behavior of a negative Poisson's ratio. Evans and Alderson [4] coined the term "auxetic materials" for substances with a negative Poisson's ratio, derived from the Greek word “*auxetos*”, meaning “that which can be increased”. This term was introduced to simplify the phrase “material with a negative Poisson's ratio”.

Such materials possess a unique characteristic when subjected to stress. Unlike conventional materials, auxetic structures and materials deform in a distinct manner under unidirectional forces such as tension and compression. When subjected to such forces, auxetic materials deform in a way that both axis dimensions undergo changes in the direction of the applied force. In contrast, conventional materials deform in a manner where one dimension changes in the same direction as the force, while the other dimension changes in the opposite direction. Figure 1 illustrates this concept.

In Fig. 1a, a honeycomb cell is subjected to lateral compression. As it is a conventional structure, it reacts with an increase in the vertical direction. In Fig. 1b, the behavior of an auxetic structure is depicted, where, when subjected to lateral tension, it expands in the vertical direction. In Fig. 1a, a non-auxetic material is presented, which, when subjected to lateral tension, compresses in the vertical direction. Figure 1b represents an auxetic material, exhibiting volumetric expansion when subjected to lateral tension.

According to Wu et al. [21], the main benefits in properties of auxetic structures, compared to conventional structures, include: Higher energy absorption, Improved hardness;—Elevated shear modulus and Greater fracture resistance. It is essential to clarify the difference between auxetic material and auxetic structure. Auxetic materials are those with a natural auxetic behavior, based on the assumption that their cells have a negative Poisson's ratio. On the other hand, an auxetic structure is one that can be constructed from an auxetic or non-auxetic material; however, the structure exhibits auxetic behavior due to its geometry derived from the unit cells.

There are different types of auxetic cells, and their classifications are numerous. However, according to Wu et al. [21] and Gill [5], the most common types of auxetic cells are: Honeycomb cells, Reentrant cells; Chiral cells; Origami cells; Star cells; Missing-rib cells. Within the domain of chiral cells, three types are defined: Anti-chiral, Chiral, and Meta-chiral. Figure 2 provides examples of chiral cells.

Anti-chiral structures consist of interconnected nodes arranged to produce a chiral (twisting) response under mechanical stress, resulting in significant flexibility and adaptability due to the specific rotation and translation of their components. Chiral structures also exhibit a twisting response but differ from anti-chiral structures

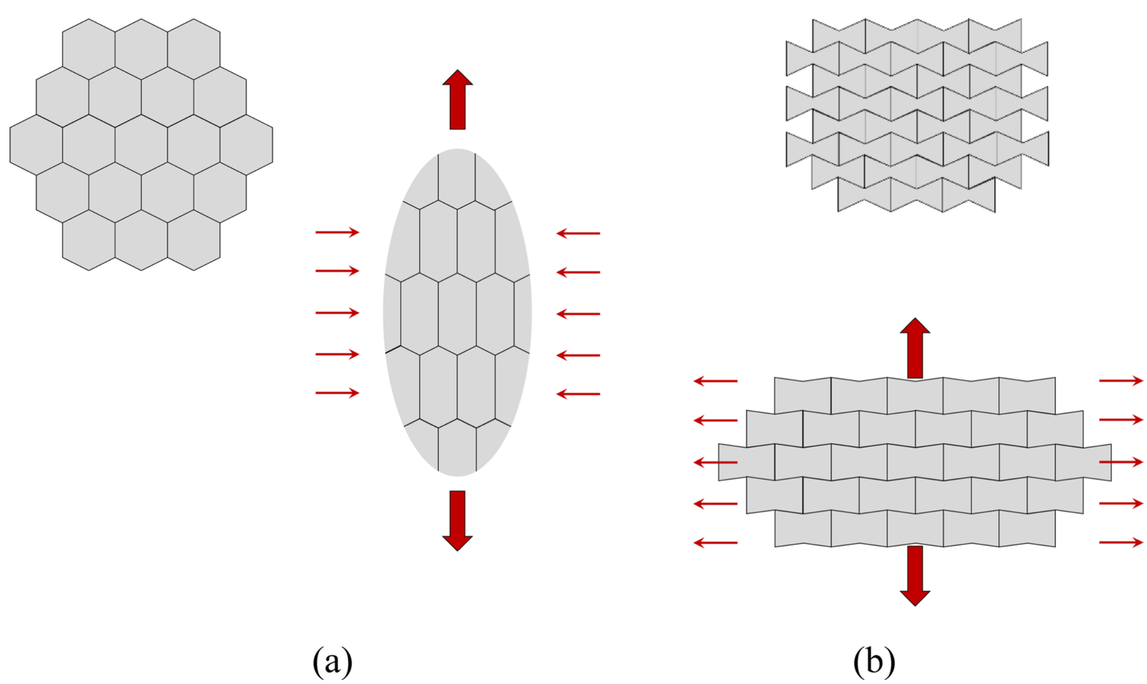

Fig. 1 Difference between non-auxetic/conventional structures and auxetic structures. **a** Non-auxetic (conventional) structure, and **b** Auxetic structure

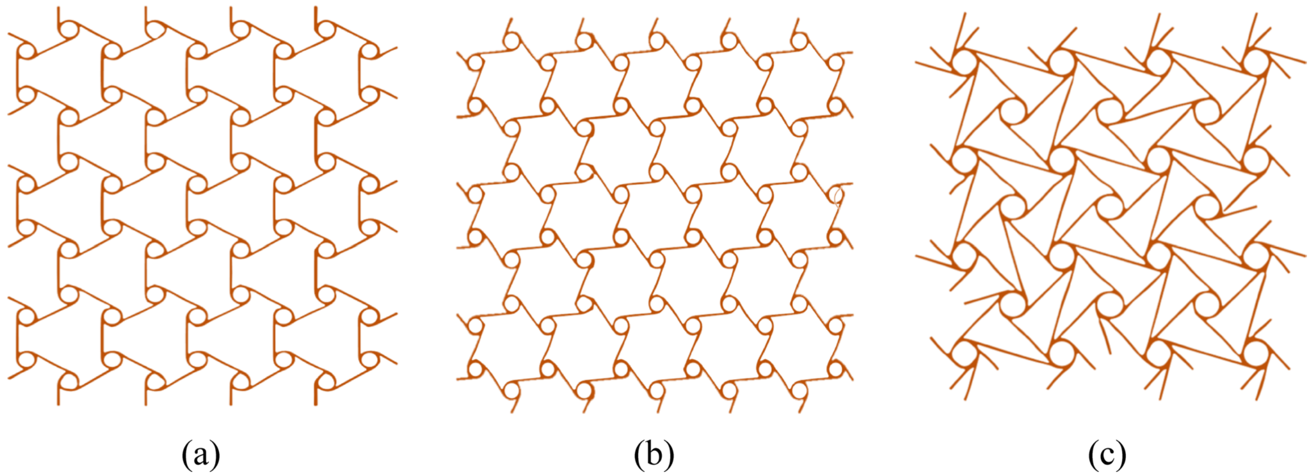

Fig. 2 Example of groups of chiral cells: **a** anti-chiral, **b** chiral and **c** meta-chiral

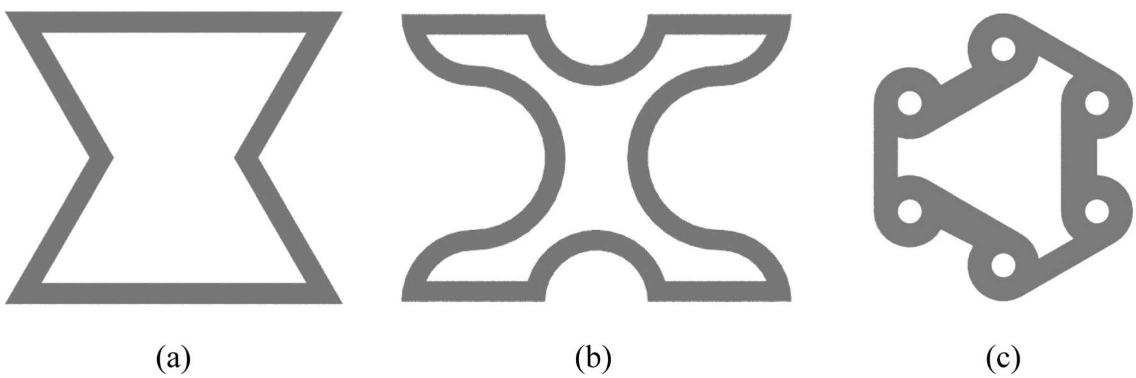

Fig. 3 Unit cells used in the study: **a** Reentrant cell, **b** Dragonfly cell, and **c** Anti-trichiral unit cells

in their symmetrical arrangement, allowing for specific directional mechanical properties, suitable for applications requiring anisotropic responses. Meta-chiral structures, a more complex form of chiral structures, have an additional hierarchical organization, exhibiting chiral behavior at multiple scales and providing enhanced mechanical properties such as increased stiffness and strength, allowing for fine-tuning of mechanical responses and adaptability to various engineering applications.

For the present study, the selection of auxetic unit cells followed the more traditional models commonly cited in the literature. These traditional models typically exhibit well-documented auxetic behavior, making them suitable for comparative analysis.

The Reentrant model, known for its characteristic reentrant geometry, serves as an excellent baseline due to its well-documented mechanical properties and predictable auxetic response. The Dragonfly model, a novel auxetic structure proposed by Gomes et al. [6], incorporates unique geometric features expected to enhance its auxetic behavior and mechanical performance. The anti-trichiral model, characterized by its chiral geometry, is included to explore the effects of chiral geometry on mechanical properties, providing a comparison to non-chiral designs like the

Table 1 Parameters for the development of auxetic tubes

Variable	Value	Unit
External diameter	91.68	mm
Internal diameter	83.68	mm
Length	85.20	mm
Edge thickness	0.60	mm
No. of cells (horizontal)	24	–
No. of cells (vertical)	6	–
Thickness between cells	2	mm

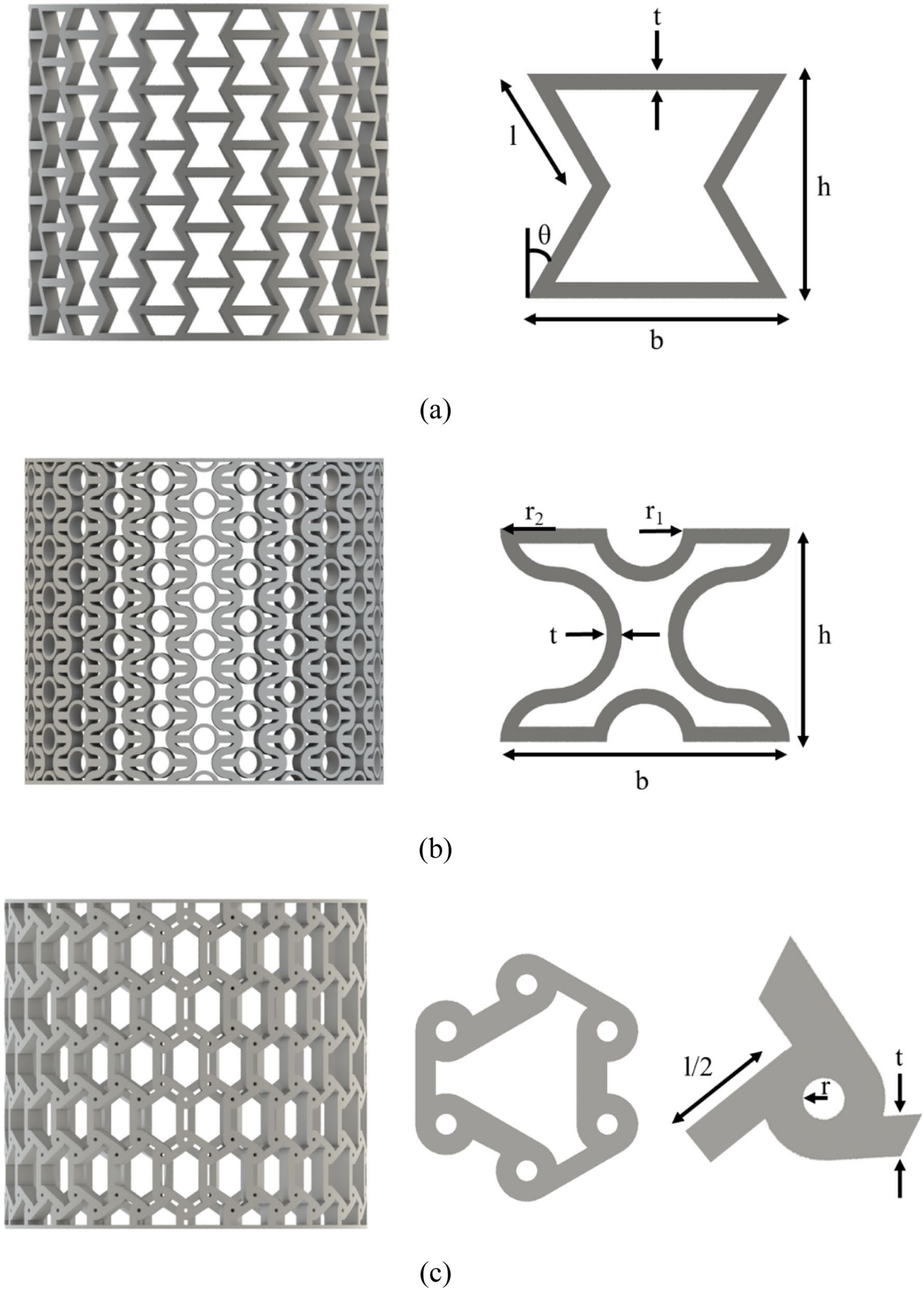

Fig. 4 Models of auxetic tubes and their unit cells: **a** Reentrant (baseline), **b** Dragonfly and **c** Anti-trichiral models

Table 2 Parameters used to print the models

Parameter	Value	Unit
Printing temperature	210	°C
Bed temperature	60	°C
Printing speed	30	mm/s
Layer height	0.2	mm
Fill density	100	%
Printing material	PLA	–

Reentrant model. By selecting these diverse structures, we aim to investigate a range of behaviors and properties exhibited by auxetic structures, enabling comprehensive analysis and comparison.

Additionally, in alignment with the parameters for 3D printing, the choice was made to align the auxetic unit cells in the current study on auxetic tubes filled with PU foam with another study on unfilled auxetic tubes. This approach ensures that the printed tubes will exhibit consistent characteristics across both studies, both in terms of auxetic unit cells and within the realm of additive manufacturing, thus enabling direct comparison. Figure 3 provides a sketch of the adopted unit cells in this study.

3 Experimental methodology

3.1 Computational modeling

The computational modeling in this study refers exclusively to the geometric parametrization conducted using CAD software, specifically SolidWorks®. This involved defining and adjusting the geometric parameters of the auxetic unit cells to ensure precise and accurate modeling of the structures. Table 1 presents the dimensions used for the tube development.

It is worth noting that these parameters were defined based on to facilitate a comparison between the two projects. For a clearer visualization of the auxetic tubes to be printed, Fig. 4 provides a section of the three types of models studied in this work, emphasizing the adopted unit cells.

As mentioned in the previous steps, it is necessary to define certain parameters for the 3D printing of the auxetic tubes that will be tested. The number of parameters is extensive, so the basic configuration adopted by Ultimaker CURA® 4.11.0 will be used. However, some other parameters were modified to enable a later comparison between the current study on foam-filled auxetic tubes and another study on unfilled auxetic tubes, using the same printing parameters. Table 2 presents the modified settings in Ultimaker CURA®.

3.2 Manufacturing

The tube prints followed the parameters described in the previous section. Once the models were set in the CURA® software, it is possible to estimate a preview of the printing time for the auxetic tubes, which are 9 h, 13 h, and 11 h for the Reentrant cell, Dragonfly cell, and Anti-trichiral cell models, respectively. Figure 5 illustrates the process of printing the auxetic tubes.

Following the timeline of 3D printing, once the auxetic tubes are printed, careful cleaning and sanding are necessary. The purpose of cleaning and sanding is to provide a better finish to the piece and to prevent any interference from residual prints, such as the previously mentioned strings, in the results of the mechanical tests. Finally, with a smooth finish and free of imperfections, it is possible to insert the polyurethane into the auxetic tube. For this, a cut PVC (polyvinyl chloride) tube was used as a boundary for the PU, as shown in Fig. 5.

With the curing time, the liquid becomes a foam, as can be seen in Fig. 6, which shows an example of an auxetic tube filled with PU foam cut in half.

3.3 Experimental setup

For the compression test on the final structure, the ASTM D695-10 standard will be followed, with a constant compression speed parameter of 2 mm/min. The location where the tests were conducted is shown in Fig. 7. In addition, the Figure shows the auxetic tubes filled with polyurethane foam inserted into the compression machine, just before the test.

With the compression test results, it was possible to plot force versus displacement curves, and from these curves, the maximum force and absorbed energy were obtained. These properties allowed for a discussion about the relationship between the increase in absorbed energy and the gain in mass.

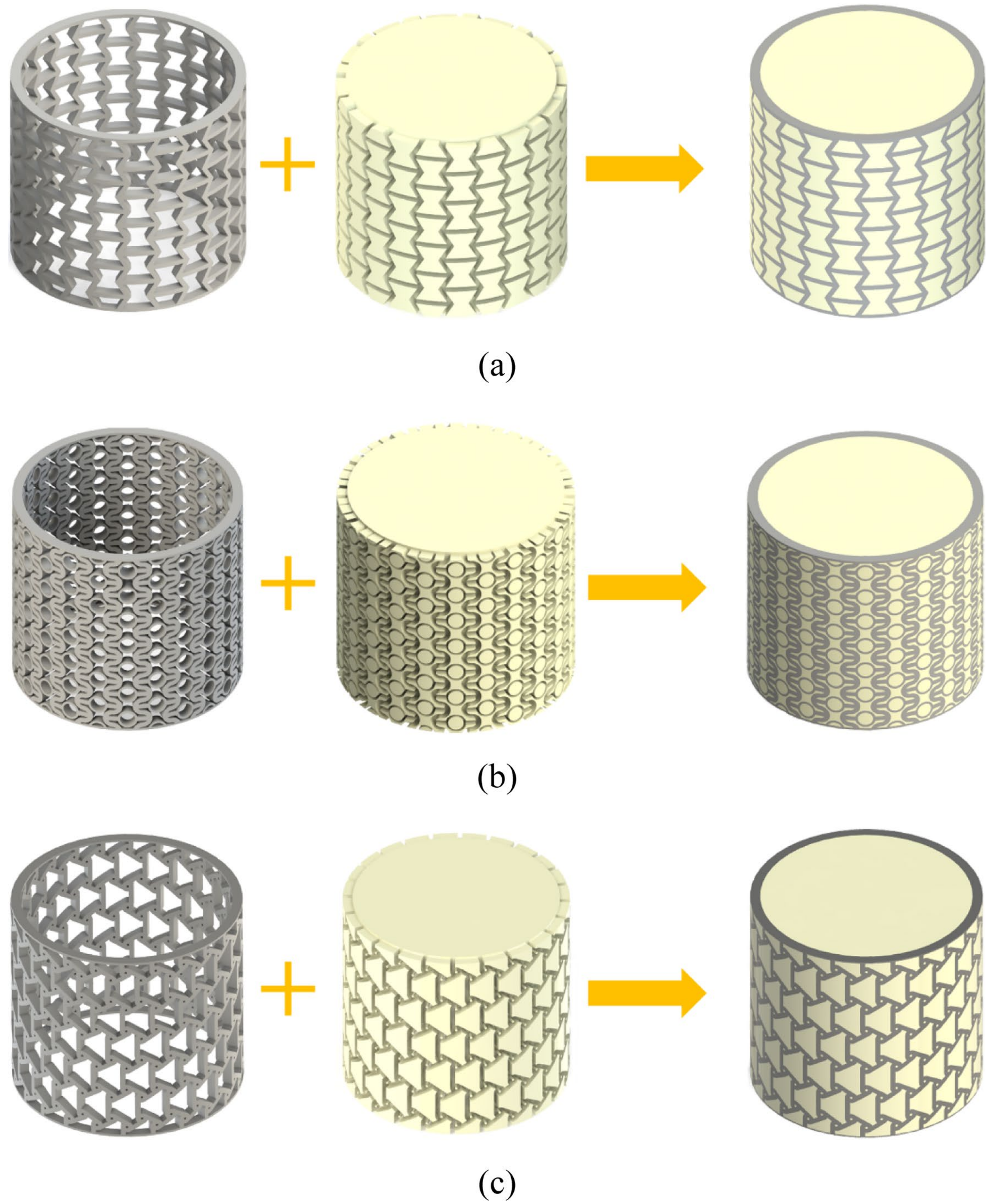

Fig. 5 Integration of auxetic tube and polyurethane for the **a** reentrant, **b** dragonfly and **c** anti-trichiral models

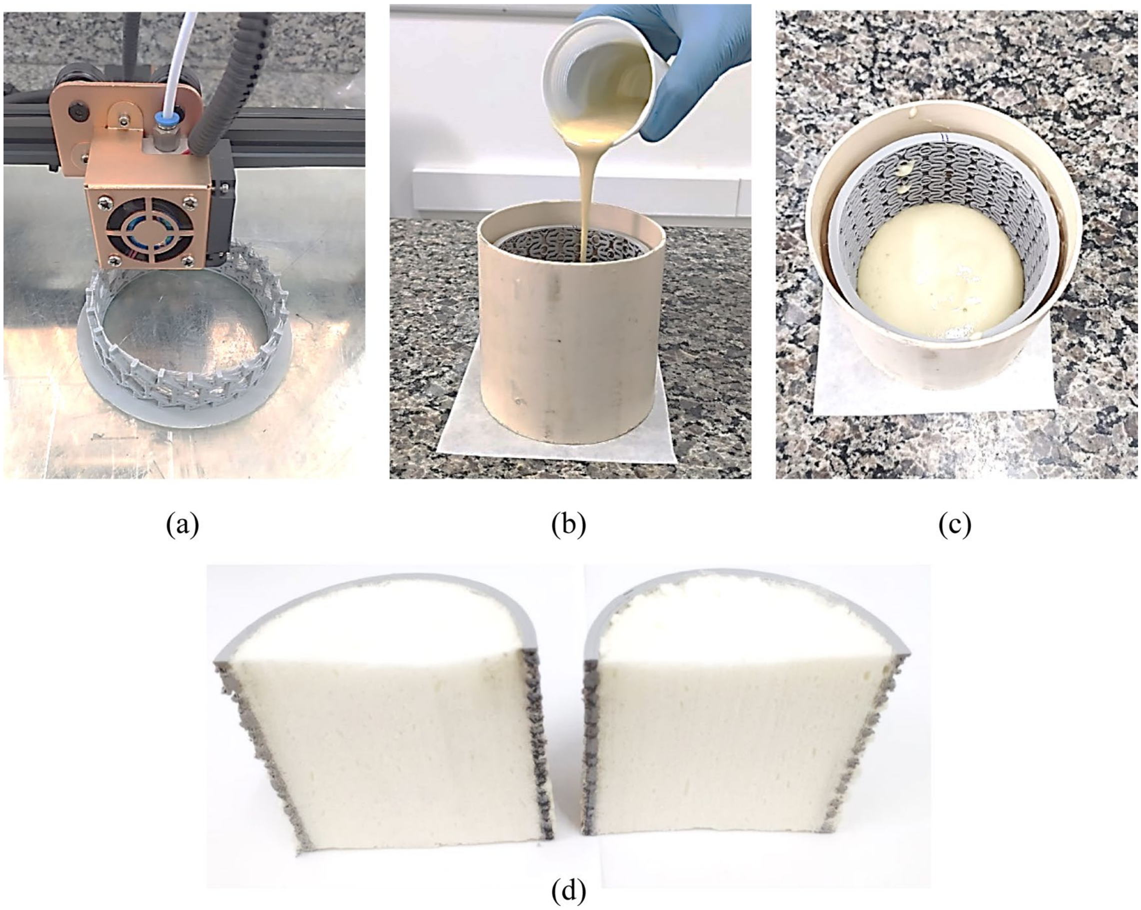

Fig. 6 Printing process, manufacturing, and details of auxetic tube

4 Results and discussion

4.1 Hybrid auxetic tube manufacturing

Three tubes were printed for each auxetic configuration: three tubes with reentrant cells (defined as conventional of baseline structure), three tubes with anti-trichiral cells, and three tubes with dragonfly cells, totaling nine tubes with auxetic structures to be filled with polyurethane foam. Figure 8 presents the fabricated tubes without and with filling, and then the masses of the three tubes subsequently.

The first analysis focused on the increase in mass due to the polyurethane filling of the auxetic tubes. As detailed in Table 3, the average weight of the unfilled reentrant-type tubes is 41.49 g, while the filled reentrant-type tubes average 60.58 g, reflecting a 46% increase in mass. For the anti-trichiral-type tubes, the average weight is 45.13 g unfilled and 67.37 g filled, indicating a 49.3% increase in mass. The dragonfly-type auxetic tubes show an average weight of 56.43 g unfilled and 78.16 g filled, with an average mass increase of 38.5%. These values highlight the significant impact of polyurethane filling on the overall mass of the auxetic tubes.

4.2 Compression test results

In this section, the curves of each auxetic structure, both unfilled and filled, will be presented separately. Additionally, an energy-based analysis will be provided through the curves of Energy Absorption versus Displacement. Figure 9 illustrates the behavior of the auxetic tubes during the compression test.

Figure 9 illustrates the microscopic view of the PLA + PU interface (a) and the PU foam only (b). In Fig. 10a, it is evident that the polyurethane is well impregnated within the auxetic structure during the manufacturing process, ensuring strong adhesion and integration between the PLA and PU. Figure 10b shows the PU foam, highlighting its closed-cell cellular structure, which contributes to the material's enhanced energy absorption and compressive strength. This detailed microscopic analysis is essential to understanding how the polyurethane filling improves the mechanical

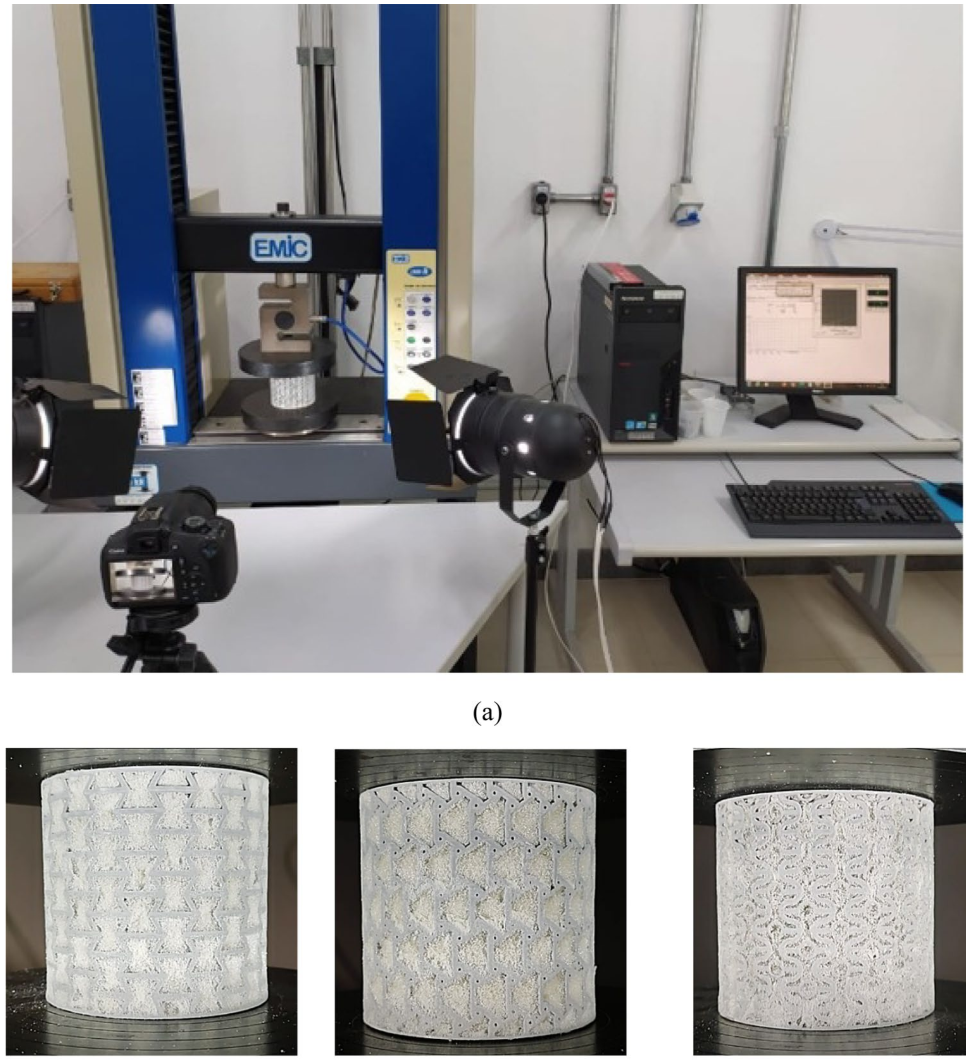

(a)

(b) Reentrant (c) Anti-trichiral (d) Dragonfly

Fig. 7 Experimental setup of the testing machine and auxetic tubes on the compression testing machine

properties of the auxetic tubes by providing additional support and energy absorption capabilities.

During the manufacturing process, the foam penetrates inside the unit cells, significantly affecting the compressive behavior of the structure. The penetration of the foam provides additional support and energy absorption, enhancing the overall compressive strength and stability. This interaction distributes the compressive forces more evenly, reducing localized stress concentrations and improving the load-bearing capacity.

Initially, with the responses from the compression tests, it was possible to draw the Force versus Displacement of the three structures studied, both with and without polyurethane foam filling. Figure 11 shows the curves for the three structures: Reentrant, Anti-trichiral and Dragonfly, respectively.

Notably, the dragonfly structure exhibited more repeatable results compared to the reentrant and trichiral structures. This variation in repeatability can be attributed to differences in the geometry of the auxetic cells. The dragonfly structure, characterized by its novel design proposed by Gomes et al. [6], likely promotes a more uniform distribution of stress and deformation, resulting in consistent performance across repeated tests. In contrast, the reentrant and trichiral structures, especially the latter with its more complex geometry, exhibited greater variability. This can be partially explained by the interaction between the PU foam and the open auxetic cells. The foam may penetrate differently in each sample, leading to variations in the internal stress distribution and, consequently, in the force–displacement behavior. The open-cell nature of the reentrant and anti-trichiral structures might also contribute to these differences, as the interaction between the foam and the structure can vary significantly between tests.

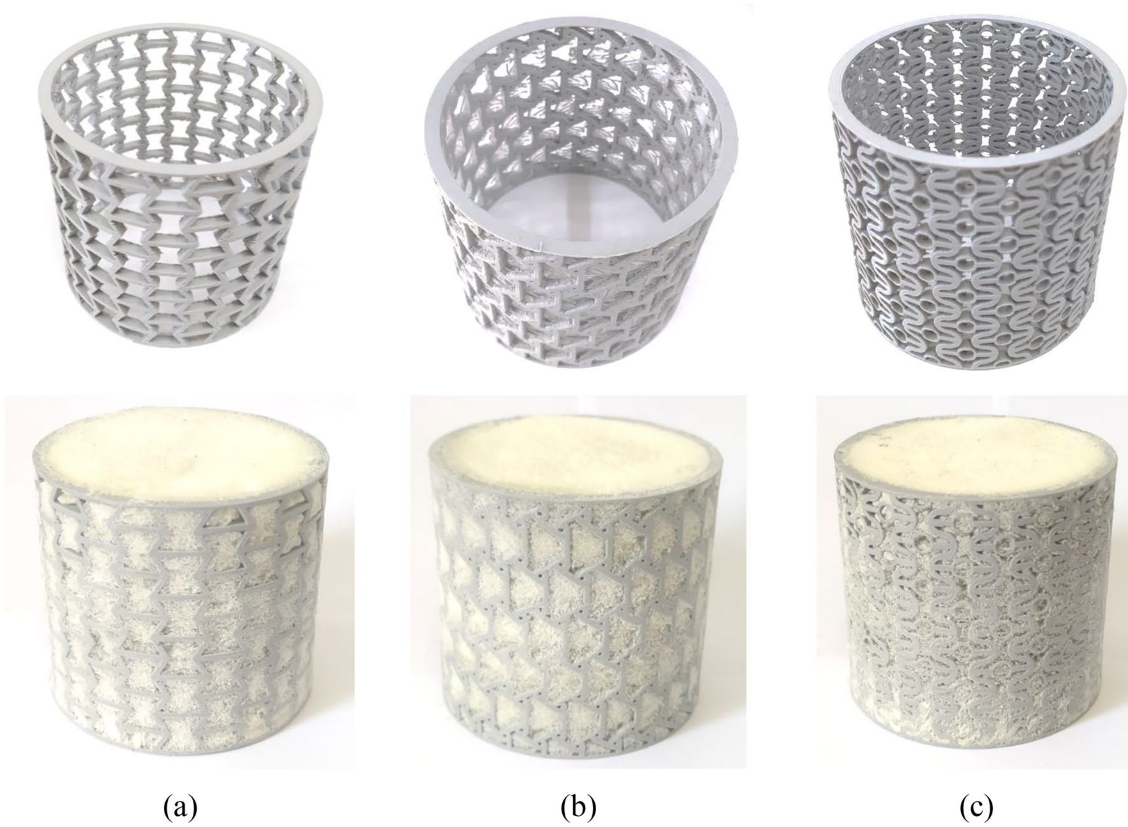

Fig. 8 Auxetic tubes without and with filling

Table 3 Masses (in grams) of reentrant, anti-trichiral, and dragonfly-type auxetic tubes

Spec	Reentrant			Anti tri-chiral			Dragon-fly		
	m	m_{PU}	Δm (%)	m	m_{PU}	Δm (%)	m	m_{PU}	Δm (%)
I	41.89	67.31	60.7	45.06	65.11	44.5	56.21	77.74	38.3
II	41.48	52.90	27.5	44.95	71.04	58.0	56.33	78.69	39.7
III	41.09	61.54	49.7	45.37	65.98	46.2	56.76	78.06	37.5
avg	41.49	60.58	46.0	45.13	67.37	49.3	56.43	78.16	38.5

In addition, observing the curves, it is immediately evident that there is a significant increase in the force required to rupture the structure with PU filling. This increase is attributed to the interaction between the auxetic structure and the PU foam. When the auxetic structure is compressed, it induces lateral expansion in the foam, which, in turn, provides additional resistance. Thus, there is a compensatory effect between the compressive forces of the auxetic structure and the lateral expansion forces of the foam. Figure 12 visually illustrates this interaction.

Similarly, a behavior of Negative Poisson's Ratio (NPR) was observed and predicted based on the compression test frames shown in Fig. 8, where the structure does not undergo significant horizontal deformation. Additionally, the Force versus Displacement curve for the anti-trichiral structure presents several peaks, which are characterized by the sequential rupture of the anti-trichiral cells. Furthermore, the dragonfly structure exhibited behavior close to ZPR, likely due to the compensating force of the foam reducing the NPR characteristic. Moreover, a sharp drop in the compression force was observed, indicating the total rupture of the auxetic structure.

Figure 13 illustrates the energy-displacement curves for the reentrant, anti-trichiral, and dragonfly (DF) structures, both with and without PU filling. The purpose of this figure is to provide a detailed analysis of the energy absorption characteristics of the different auxetic structures under compression. While the force–displacement curves in Fig. 10 demonstrated that a higher compressive force is required to deform the structures filled with PU, Fig. 13 highlights

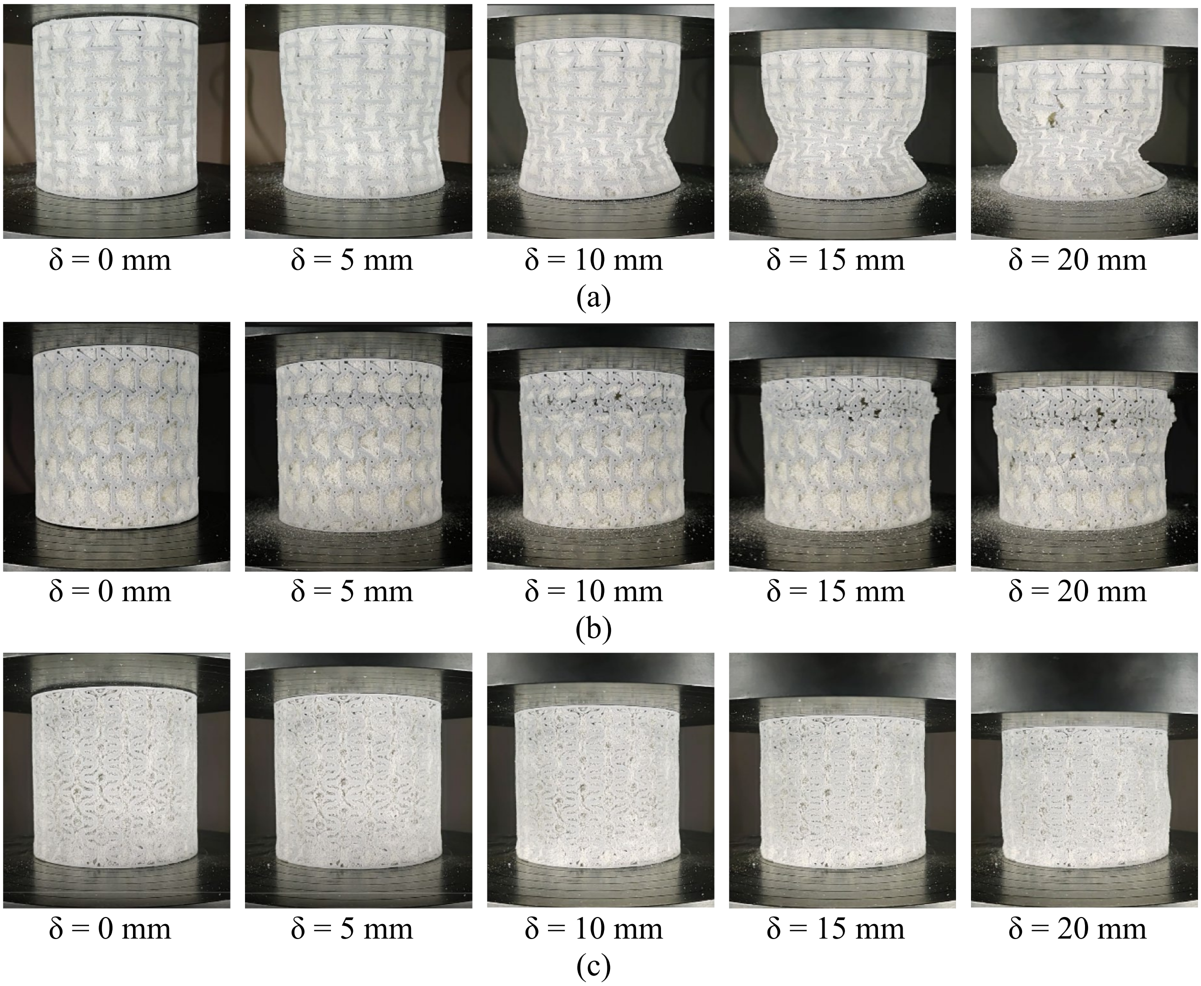

Fig. 9 Behavior of auxetic tubes during the quasi-static compression test. The frames correspond to fixed displacement intervals (δ)

the total energy absorbed by the structures during deformation. This additional perspective is crucial for understanding the improvements in energy absorption and the overall mechanical performance of the auxetic structures due to the PU filling.

With the above curves, it confirms what was analyzed earlier: for the auxetic tubes filled with foam, a significantly higher compressive force is required to rupture the structure compared to the tube with the same auxetic structure but without filling. For better visualization, the Energy Absorbed per Displacement curves for the auxetic tubes with and without filling was plotted separately, as shown in Fig. 14.

In Fig. 14a, which shows the energy-displacement curves for the unfilled auxetic tubes, we observe that the dragonfly structure exhibits the highest energy absorption, followed by the trichiral and reentrant structures. This behavior is expected due to the intrinsic geometric advantages of the dragonfly design, which allows for better distribution and absorption of energy under deformation.

Equally important, Fig. 14b shows the energy-displacement curves for the auxetic tubes filled with PU. Here, we see a significant increase in energy absorption for all structures compared to their unfilled counterparts. The dragonfly structure continues to demonstrate superior performance, with the highest energy absorption. The trichiral and reentrant structures also show considerable improvements in energy absorption, indicating the beneficial effects of PU filling.

These curves illustrate the enhanced mechanical performance of the auxetic structures when filled with PU. The PU filling not only increases the energy absorption capacity but also provides additional support, reducing localized stress concentrations and improving the overall load-bearing capacity of the structures. This behavior aligns with our expectations, as the interaction between the PU foam and the auxetic structures is designed to maximize energy absorption and mechanical stability.

For a clearer interpretation of the results, Table 4 summarizes all the values found and calculated previously,

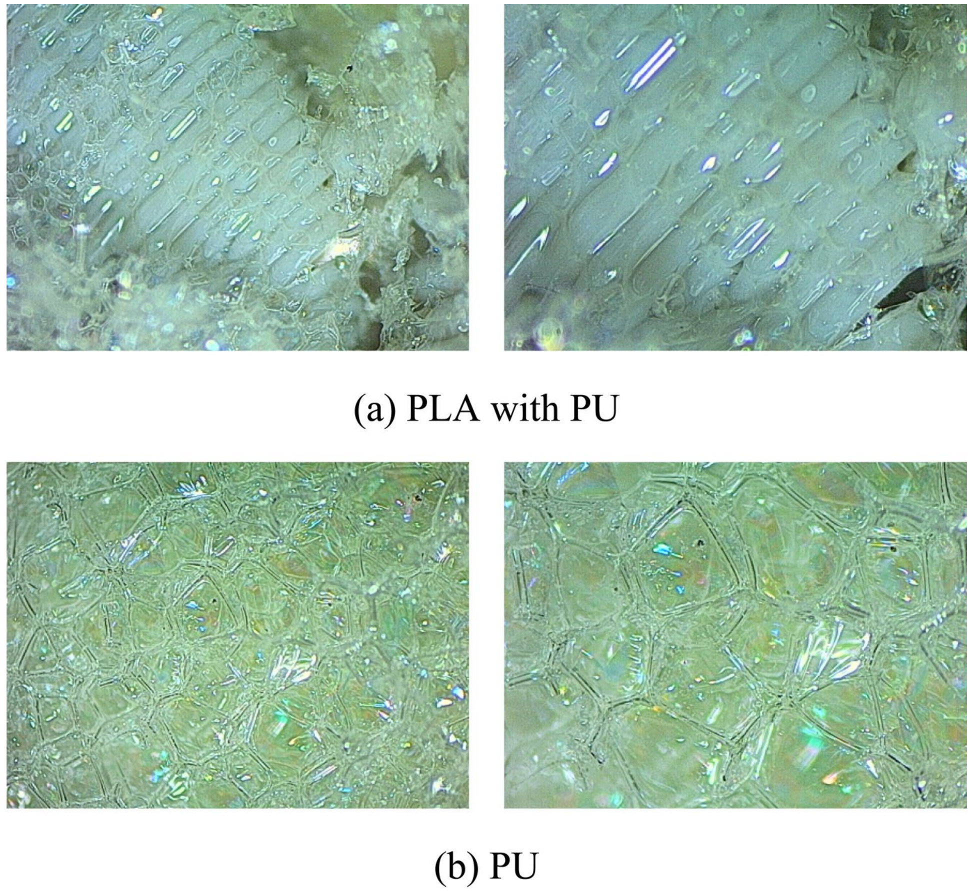

Fig. 10 Microscopic view of PLA + PU interface (**a**) and PU only (**b**)

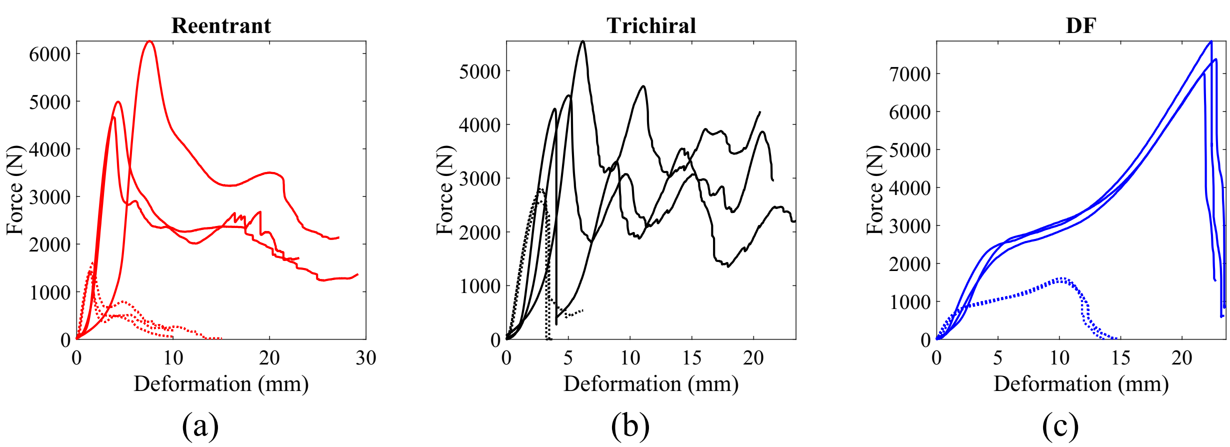

Fig. 11 Force–displacement curves (dashed line no PU, solid line with PU)

including the maximum force, specific force, and Main Crush Force (MCF) for each studied auxetic tube. The MCF is determined by the absorbed energy per displacement. On average, for the reentrant structure, a 1% increase in mass results in a 23.59% increase in specific absorbed energy. For the anti-trichiral and dragonfly structures, a 1% increase in mass results in a 17.65% and 15.56% increase in specific absorbed energy, respectively.

The manufacturing process used in this study, specifically FDM with PLA, provided the flexibility to create complex auxetic structures. The interface between the PLA and PU foam was found to be strong, with the PU

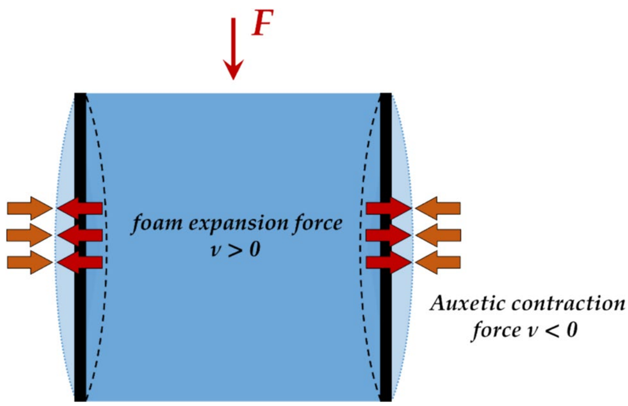

Fig. 12 Compensating forces of the PU foam and the auxetic tube

effectively penetrating the PLA structure. This interaction significantly enhanced the mechanical properties of the composite material. While FDM was suitable for this study, other AM techniques like SLS or SLA could offer advantages in surface finish and dimensional accuracy, though they may involve higher costs and different challenges. Addressing these manufacturing considerations is crucial for optimizing the performance and applicability of auxetic structures in various industrial sectors.

With the values from Table 4, it was possible to generate spider plot graphs, which aim to bring information about the properties of the structures in a visually simple format for comparisons. Figure 15 presents a comparison between the specimens without and with filling, but which have the same auxetic structure. Figure 16, on the other hand, presents a comparison between auxetic structures, evaluating the type of filling separately.

Regarding the results, there was an increase in specific absorbed energy, with an average increase in 6.3. Additionally, it was observed that the reentrant auxetic

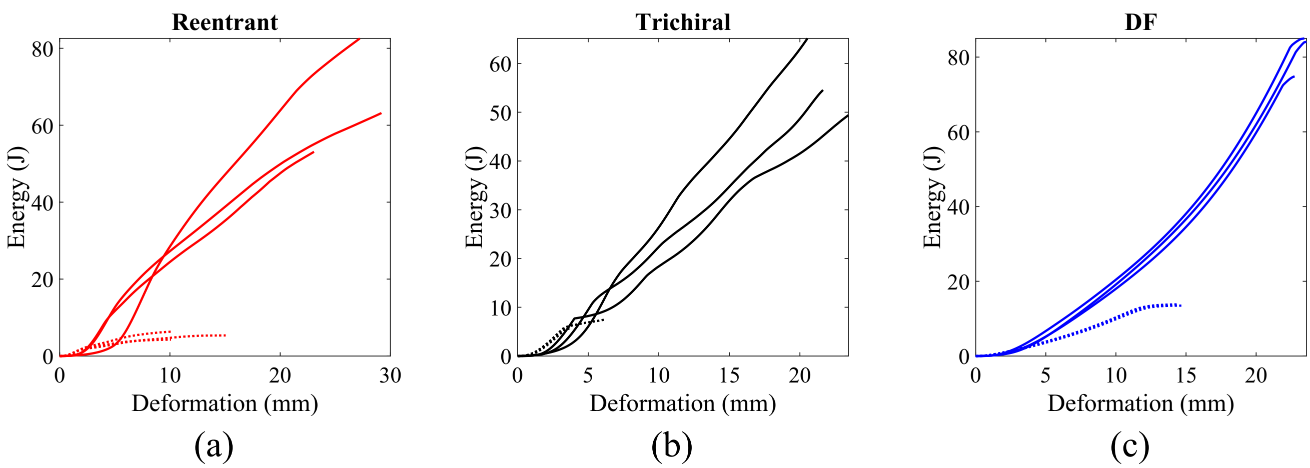

Fig. 13 Energy-displacement curves (dashed line no PU, solid line with PU)

Fig. 14 Energy versus displacement—auxetic tubes with and without filling

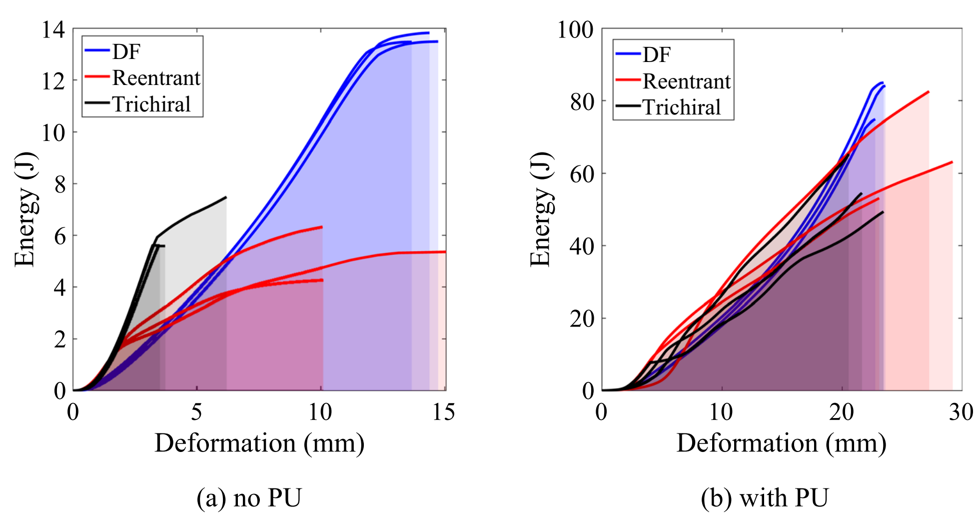

Table 4 Summary of results found

Core	Structure	Mass (g)	Disp. (mm)	Force (N)	Spec. *F*. (N/g)	EA (J)	SEA (J/g)	MCF (N)
No	Reentrant	41.49	11.74	1490	35.91	5.51	0.13	0.47
	Anti-trichiral	45.13	5.80	2714	60.14	5.84	0.13	1.01
	Dragonfly	56.43	14.26	1555	27.56	13.52	0.24	0.95
Yes	Reentrant	60.58	26.50	5304	87.55	65.34	1.08	2.46
	Anti-trichiral	67.37	21.90	4794	71.16	56.67	0.84	2.59
	Dragonfly	78.16	23.26	7412	94.83	81.00	1.04	3.48

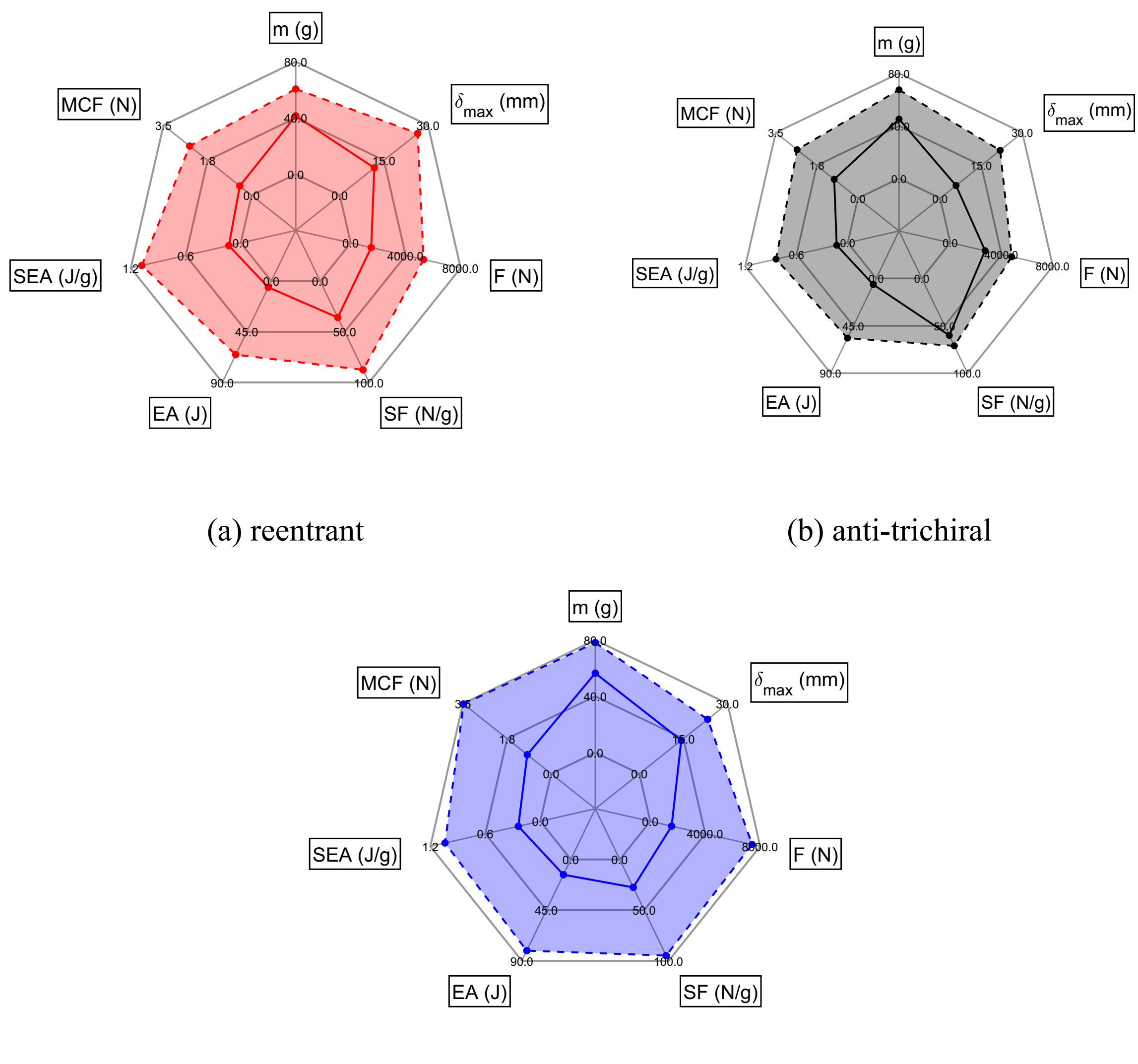

(a) reentrant

(b) anti-trichiral

(c) dragonfly

Fig. 15 Graphical visualization of structure properties (legend: dashed line without PU solid line with PU)

tube achieved the best specific absorbed energy (J/g) and incremental ratio, reaching values of 1.08 J/g and 23.59, respectively. However, the highest MCF is assigned to the dragonfly structure with PU filling, reaching a value of 3.48 N, which is 3.66 times higher than its result without filling.

It was also observed that the dragonfly structure with polyurethane filling had the highest values in 5 out of the 7 evaluated properties, lacking only maximum displacement

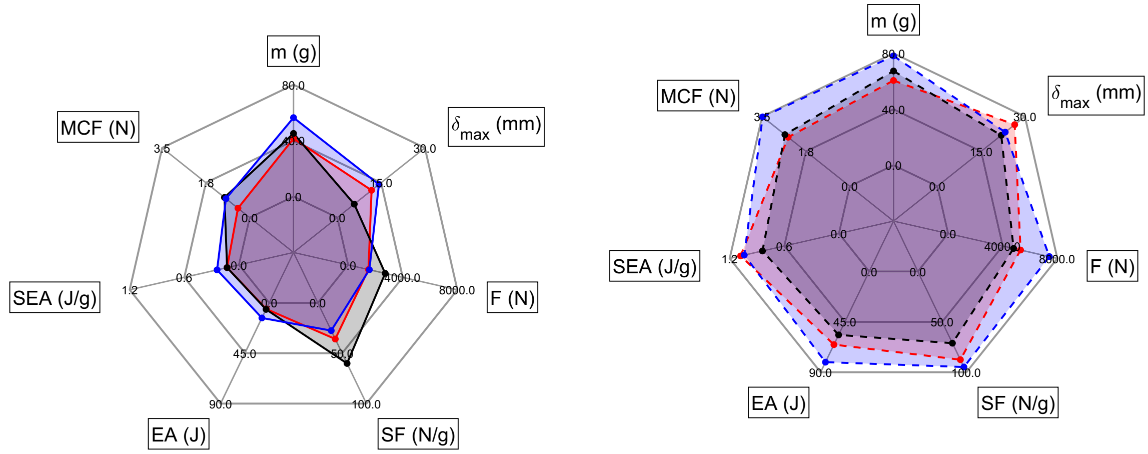

(a) no PU

(b) with PU

Fig. 16 Graphical visualization of the properties of structures without and with PU (legend: red solid line reentrant, block solid line anti-trichiral, blue solid line dragonfly)

and specific absorbed energy. Conversely, its structure without filling has higher values in only 2 out of the 7 properties: specific force and maximum force. These observations lead to the conclusion that the dragonfly structure shows greater benefits with PU filling than the other two structures.

Different behaviors than expected were observed for the anti-trichiral and dragonfly structures. The anti-trichiral structure exhibited ZPR behavior, with no positive or negative bulging horizontally, thus experiencing linear deformation and rupture of the unit cells. This behavior shows compression force peaks, characterized by the rupture of the unit cells. The dragonfly structure exhibited an inconclusive behavior, but close to that of ZPR as well. This may be due to the compensation of the foam force, reducing the NPR behavior of the dragonfly structure. Its behavior characterizes a single peak of compression force, leading to a force drop due to the complete rupture of the structure. However, even with these behaviors, an increase in the specific absorbed energy ratio for the anti-trichiral and dragonfly structures was verified.

5 Conclusions

In this study, concepts of Additive Manufacturing and Auxetic Structures were presented, highlighting their implementation advantages. Both topics are in constant evolution and development, demonstrating their extensive applicability. However, as these subjects are undergoing constant and accelerated development, the current market has not fully embraced the new production and application models. Thus, fine-tuning and integration of these concepts into the current market, which are becoming increasingly promising, are necessary.

Concerning the production of auxetic tubes, there is ease in their fabrication due to additive manufacturing. However, there was no optimization study of printing parameters to determine the best configuration for printing, leading to minor flaws and defects in the printing of auxetic tubes. Such imperfections may interfere with the results, but on an insignificant scale.

This study confirms the increase in the mechanical rigidity of the auxetic structure through PU filling, without a significant increase in its structural weight, thus achieving its central objective. Furthermore, all specific objectives were achieved, enabling the accomplishment of the main objective of the work.

To complement this study, a thorough investigation into the anti-trichiral and dragonfly structures, starting with additive manufacturing, is recommended. Such an investigation will allow for concrete conclusions about the behaviors of these auxetic structures. Additionally, a study on the optimization of printing parameters would be beneficial to obtain better and more grounded results. Moreover, an analysis of the efficiency of auxetic structures with PU core on a larger scale can yield interesting results for the development of the subject. Exploring potential applications of filled auxetic structures in different engineering sectors is also suggested.

References

1. Abeykoon C, Sri-Amphorn P, Fernando A (2020) Optimization of fused deposition modeling parameters for improved PLA and ABS 3D printed structures. Int J Lightw Mater Manuf 3:284–297
2. Airoldi A, Novak N, Sgobba F, Gilardelli A, Borovinšek M (2020) Foam-filled energy absorbers with auxetic behaviour for localized impacts. Mater Sci Eng A 788:139500
3. Batkuldinova K, Abilgaziyev A, Shehab E, Hazrat Ali M (2021) The recent development of 3D printing in developing lower-leg exoskeleton: a review. Mater Today Proc 42:1822–1828
4. Evans EK, Alderson A (2000) Auxetic materials: functional materials and structures from lateral thinking. Adv Mater 12(9):617–628
5. Gill HS (2020) Mechanical and structure properties of cellular auxetic materials. Mater Today Proc 37(2):3320–3323
6. Gomes RA, Oliveira LA, Francisco MB, Gomes GF (2024) A novel dragonfly wing shape auxetic tubular structure with negative Poisson's ratio. Smart Mater Struct (in press)
7. Huang TT, Ren X, Zeng Y, Zhang Y, Luo C, Zhang XY, Xie YM (2021) Based on auxetic foam: a novel type of seismic metamaterial for Lamb waves. Eng Struct 246:112976
8. Jiang L, Hu H (2016) Low-velocity impact response of multilayer orthogonal structural composite with auxetic effect. Compos Struct 169:62–68
9. Jin X, Wang Z, Ning J, Xiao G, Liu E, Shi X (2016) Dynamic response of sandwich structures with graded auxetic honeycomb cores under blast loading. Compos Part B 106:206–217
10. Jopek H (2016) Computer simulation of bending a fibrous composite reinforced with auxetic phase. Phys Status Solidi B 253(7):1369–1377
11. Jopek H (2017) Finite element analysis of tunable composite tubes reinforced with auxetic structures. Materials 10(12):1359
12. Lakes R (1987) Foam structures with a negative Poisson's ratio. Science 235(4792):1038–1040
13. Liu J, Yang W, Liu J, Liu J, Huang W (2023) Ballistic impact analysis of foam-filled double-arrow auxetic structure. Thian Wall Struct 182:110173
14. Mohanavel V, Ali KSA, Ranganathan K, Jeffrey JA, Ravikumar MM, Rajku S (2021) The roles and applications of additive manufacturing in the aerospace and automobile sector. Mater Today Proc 47(1):405–409
15. Mohsenizadeh S, Alipour R, Rad MS, Nejad AF, Ahmad Z (2015) Crashworthiness assessment of auxetic foam-filled tube under quasi-static axial loading. Mater Des 88:258–268
16. Novak N, Starčevič L, Vesenjaka M, Ren Z (2019) Blast response study of the sandwich composite panel with 3D chiral auxetic core. Compos Struct 215:167–178
17. Paolini A, Kollmannsberger S, Rank E (2019) Additive manufacturing in construction: a review on processes, applications, and digital planning methods. Addit Manuf 30:100894–100907
18. Ren X, Zhang Y, Han CZ, Han D, Zhang XY, Zhang XG, Xie YM (2022) Mechanical properties of foam-filled auxetic circular tubes: experimental and numerical study. Thin Wall Struct 170:108584
19. Wang Y, Wang L, Ma Z, Wang T (2016) Parametric analysis of a cylindrical negative Poisson's ratio structure. Smart Mater Struct 25(14):35038
20. Wang Z, Zulifqar A, Hu H (2016) Auxetic composites in aerospace engineering. In: Advanced composite materials for aerospace engineering, pp 213–240
21. Wu W, Hu W, Qian G, Liao H, Xu X, Berto F (2019) Mechanical design and multifunctional applications of chiral mechanical metamaterials: a review. Mater Des 180:107950
22. Xiao R, Feng X, Fan R, Chen S, Song J, Gao L, Lu Y (2020) 3D printing of titanium-coated gradient composite lattices for lightweight mandibular prothesis. Compos B 193:108057–108067